DOI: 10.4408/IJEGE.2011-03.B-054

NUMERICAL SIMULATION OF FLOOD AND DEBRIS FLOWS THROUGH DRAINAGE CULVERT

JOONGCHEOL PAIK & SANG-DEOG PARK(*)

(*) Gangneung-Wonju National University, Department of Civil Engineering, Korea

ABSTRACT

In mountainous area, cross drainage culvert is commonly used to allow water and debris to pass underneath road or embankment. Flood and debris flows typically undergo a sudden change of the flow depth in the open channel with culvert due to the discontinuity of the bottom slope and the cross-sectional area near the culvert inlet, which can result in culvert failure due to blockage. In this study, we seek to improve our understanding of the culvert flow and its transition in such open channel. A second-order-accurate finite volume method using a shock-capturing scheme with TVD limiters has been developed for solving one-dimensional shallow water equations with debris flow resistance terms to predict the time-dependent behavior of non-Newtonian debris flow through culverts. To evaluate the numerical model, we first apply it to calculate a saturated debris flow in a large scale experimental channel. The comparison of the numerical results with experimental measurements shows that the present model can reasonably well reproduce laboratory but fairly large scale debris flows. To investigate the behaviour of the common flood flow, an immature debris flow and debris flow in our laboratory flume with a square culvert and an abrupt change of bed slope, we conducted these flows using corresponding flow resistance relations. The numerical results appear to be in good agreement with our experimental measurements which provide useful information on the debris flow transient through culverts. The numerical results show that the present model is a promising engineering tool for practical simulations of such flows. We elucidate the transient features of flood and debris flows through culverts, based on numerical solutions of such flows in the open channel with culvert at various configurations of different bottom slopes between the channel and the culvert.

KEY WORDS: *debris flow, culvert, numerical simulation*

INTRODUCTION

Over recent decades, there have been lots of efforts to understand the propagation and deposition behavior of the debris flows. Due to the huge difficulty of the real-time field measurements, the majority of debris flow researches have been carried out by laboratory experiments and numerical simulations with the parameters back-calculated or calibrated to match previous field events. The physical modeling has provided much of what we know about the rheology of the debris flow, but their results suffer from spatial scale effects and are approximately applicable to large-scale events. The numerical simulation has become an ideal approach for reproducing the debris flow propagation.

The debris can include anything from the smallest clay to boulders, trees and even parts of man-made structures. Debris flow is generally considered to contain more than 50% particles larger than sand size (VARNES, 1978) while mudflow is composed

predominantly of silt, with some clay and fine sand. Distinct physical processes differentiate these type of flows based on the rheology of the water-sediment mixture. According to Julien & Leon (2000), the yield and viscous stresses are dominant in mudflows and the dispersive stress is dominant in debris flows. The sediment concentration also can be used to distinguish between stony debris flow, immature debris flow (less than about 0.2), and turbulent flow (less than about 0.02) (Takahashi, 1991). In numerical simulations of such immature debris and debris flows, practical problems are to determine representative parameters, such as bulk viscosity and yield stress, characterizing the solid-fluid mixture and to select the appropriate flow resistance relations (Naef *et alii,* 2006). To investigate the distinct features of debris flow compared to those of common flood flow, in this study, we solved the governing equations with considering three resistance formula available for different flow regimes: 1) the turbulent flow relation for the bed load/suspended load flow; 2) the immature debris flow model (Takahashi, 1991); and 3) the Voellmy debris flow model.

In this work a 1D numerical model is developed by employing a shock capturing method, which works in the finite volume context with an approximate Riemann solver, to simulate fluid mixture (mud/debris) flows. The present model solves the time-dependent nonlinear one dimensional shallow water equations with complex source terms by the Weighted Averaged Flux (WAF) method using the HLL approximate Riemann solver, with total variation diminishing (TVD) limiters

In the subsequent section, we first present the governing equations based on the shallow water equations incorporated with various flow resistance relations to determine the basal and/or internal friction slope and the numerical methods. In Paik *et alii* (2010), the numerical model was already evaluated by applying to a dam break problem with analytical solutions accounting for a Coulomb-type behavior with constant friction angle on constant slope bottom and to a mudflow which was experimentally investigated in a small scale rectangular channel of a constant slope. In this study, we apply the present model to a debris flow experimentally reproduced in a large scale USGS flume to further evaluate its computational performance. Subsequently, we present and discuss numerical results of a flood (water) flow, an immature debris flow with relatively low sediment concentration and debris flow at the same flow rate condition. Recently, these flows had been also investigated in our laboratory channel with rectangular cross section and an abrupt slope change of the slope. Finally, conclusions about behaviour of these flows with same flow rate but different sediment concentrations in the culvert-like experimental flume are drawn

NUMERICAL MODEL

GOVERNING EQUATIONS

The shallow water equations can be applied to both dam break wave propagation and non-Newtonian mud/debris flows with an appropriate flow resistance term (Jin & Fread, 1999; Brufau *et alii*, 2000; Naef *et alii*, 2006). The continuity and momentum equations are written in the conservative form as follows:

$$\frac{\partial \mathbf{U}}{\partial t} + \frac{\partial \mathbf{F}(\mathbf{U})}{\partial x} = \mathbf{H}(\mathbf{U}) \tag{1}$$

where

$$\mathbf{U} = \begin{pmatrix} h & hu \end{pmatrix}^T$$

$$\mathbf{F}(\mathbf{U}) = \begin{pmatrix} hu \\ hu^2 + \frac{1}{2}gh^2 \end{pmatrix}$$

$$\mathbf{H}(\mathbf{U}) = \begin{pmatrix} q_l \\ gh\left(S_0 - S_f\right) \end{pmatrix}$$

In above equation, t = time; x = the distance along the longitudinal axis of the channel; h = the flow depth normal to the local bed surface; u is the depth-averaged velocity; q_l = lateral inflow or outflow; g = the gravity acceleration; S_0 = the bed slope given by the bed inclination θ

$$S_0 = \tan\theta = -\frac{\partial z}{\partial x} \tag{2}$$

where $z(x,t)$ = the bed level respect to an arbitrary horizontal reference. In this study, various flow resistance relations for the flow resistance term S f available for mud/debris flows are implemented in the model.

If the solids concentration is less than about 0.02, the flow contains bed load or suspended load depending on the turbulenceand viscosity.

$$S_f = \frac{n^2}{h^{4/3}} u|u| \tag{3}$$

where n = pseudo Manning's roughness coefficient which accounts for both turbulent boundary friction and internal collisional stresses.

$$S_f = \frac{1}{0.49 g h_r}\left(\frac{d_p}{h}\right)^2 u|u| \tag{4}$$

where $h_r = A/P$ = the hydraulic radius, P = the wetted perimeter, d_p = the mean effective diameter of particles.

The Voellmy flow relation consists of a turbulent Chézy coefficient accounting for velocity dependent friction losses and a basal friction term to describe the stopping mechanism, and presents the good behaviour regarding both the debris flow behavior and the deposit characteristics (Bertolo & Wieczorek, 2005; Naef *et alii,* 2006; Medina *et alii*, 2008).

$$S_f = \frac{q\sqrt{q^2}}{h^2 C_Z^2 h_r} + \cos\theta \tan\phi \tag{5}$$

where θ is internal friction angle of the flowing mass and C_Z is the Chézy coefficient.

NUMERICAL METHODS

The method employed in this study works in the finite volume context with an approximated Riemann solver. Using the explicit conservative formulation of the governing equations, the upwind scheme can be applied in the form

$$\mathbf{U}_i^{n+1} = \mathbf{U}_i^n - \frac{\Delta t}{\Delta x}\left(\mathbf{F}_{i+1/2} - \mathbf{F}_{i-1/2}\right)^n + \Delta t \mathbf{H}_i^n \tag{6}$$

where Δt = the time interval; Δx = the spatial step; n = the time interval index; i = the spatial node index; and $\mathbf{F}_{i+1/2}$ = the numerical flux at the cell interface $x = x_{i+1/2}$. The weighted averaged flux (WAF) method is a second-order extension of the Godunov upwind method (Toro, 2001). A total variation diminishing (TVD) constrain is enforced on the scheme to avoid spurious oscillations in the vicinity of discontinuities. The resulting TVD version of the secondorder WAF flux is

$$\mathbf{F}_{i+1/2} = \frac{1}{2}\left(\mathbf{F}_i + \mathbf{F}_{i+1}\right) - \frac{1}{2}\sum_{k=1}^{2} \mathrm{sgn}\left(c_k\right) A_k \Delta \mathbf{F}_{i+1/2}^k \tag{7}$$

where $C_k = S^k \Delta t/\Delta x$ Courant number related to the wave speed S^k ; A_k = second-order accurate WAF limiter function which, in this study, is obtained using either minmod or superbee limiter (Toro, 2001); $\Delta \mathbf{F}^k_{i+1/2}$ = flux jump across wave k :

$$\Delta \mathbf{F}_{i+1/2}^k \equiv \mathbf{F}_{i+1/2}^{k+1} - \mathbf{F}_{i+1/2}^k \tag{8}$$

The flux limiter allows one to obtain a first-order-accurate solution for the discontinuities and a second-order-accurate solution elsewhere. To determine the wave speeds and flux jumps, we employ the HLL approximate Riemann solver which is based on the estimates of the smallest and the largest wave speeds arising in the Riemann solution:

$$\begin{aligned} S_L &= u_L - a_L q_L \\ S_R &= u_R + a_R q_R \end{aligned} \tag{9}$$

where q_K(K=L;R) , is given as follows:

$$q_{L,R} = \begin{cases} \sqrt{\frac{1}{2}\frac{\left(h_* + h_{L,R}\right)h_*}{h_{L,R}^2}} & \text{if } h_* > h_{L,R} \\ 1 & \text{if } h_* \le h_{L,R} \end{cases} \tag{10}$$

The solution of the flow depth h in the star region is obtained by the approximate Riemann solver (Toro 2001):

$$h_* = \left[\left(a_L + a_R\right)/2 + \left(u_L - u_R\right)/4\right]^2 / g \tag{11}$$

The HLL numerical flux is determined as

$$\mathrm{F}_{i+1/2} = \begin{cases} \mathbf{F}_L & \text{if} \quad S_L \ge 0 \\ \mathbf{F}^{HLL} & \text{if} \quad S_L \le 0 \le S_R \\ \mathbf{F}_R & \text{if} \quad S_R \le 0 \end{cases} \tag{12}$$

where $\mathbf{F}^{HLL} = \dfrac{S_R \mathbf{F}_L - S_L \mathbf{F}_R + S_R S_L \left(\mathbf{U}_R - \mathbf{U}_L\right)}{S_R - S_L}$.

The approximate Riemann solver offers a simple way of dealing with dry bed conditions and the determination of the wet/dry frontvelocities (Toro, 2001). The wave speeds are determined as the exact dry front speeds as follows:

$$S_L = \begin{cases} u_R - 2\sqrt{gh_R} & \text{if } (h_L = 0,\ h_R > 0) \\ u_L - \sqrt{gh_L} & \text{if } (h_L > 0,\ h_R = 0) \end{cases}$$
$$S_R = \begin{cases} u_L - 2\sqrt{gh_L} & \text{if } (h_L > 0,\ h_R = 0) \\ u_R - \sqrt{gh_R} & \text{if } (h_L = 0,\ h_R > 0) \end{cases} \quad (13)$$

The solution and integration of the system of equations (1) using the fractional-step approach involves a two-step solution procedure. In the first step, only the homogeneous part of the system is solved with the HLL approximate Riemann solver. In the second step, the source term is taken into account by solving the ordinary differential equation using the first-order accurate, splitting method.

$$\frac{d\mathbf{U}}{dt} = \mathbf{H}\left(\mathbf{U}^{adv}\right) \quad (14)$$

where $\mathbf{U}^{adv}$ is the advected flow variable based on the solution of only the homogeneous part of the system. The friction term has been discretized by a full implicit method (Liang & Marche, 2009)

$$\mathbf{U}^{n+1} = \mathbf{U}^{n} + \Delta t g h \left[S_0 + \left(\frac{S_f}{D} \right) \right]^{n} \quad (15)$$

where $D = 1 - \Delta\Delta n \left(\partial S_f / \partial q^n\right)$ is the coefficient derived for a full implicit scheme.

The performance of the numerical model and the grid sensitivity of the solutions had been evaluated by comparing the numerical solutions computed on successively refined grids with analytical solutions accounting for a Coulomb-type friction law on the dry bottom of the constant slope which is higher than the internal friction slope and some experimental measurements of debris flows. Numerical tests confirm that the numerical model yields solutions in very good agreement with the analytical solutions even near the discontinuities at appropriately refined grid resolution. For a detailed description of the numerical method and its performance the reader is referred to Paik *et alii* (2010).

RESULTS AND DISCUSSION

WATER-SATURATED DEBRIS FLOWS

In order to further evaluate the applicability of the present numerical model, we first applied the numerical methods for reproducing the debris flow in a large scale USGS experimental flume which was experimentally and numerically investigated by Denlinger & Iversion (2001). The experiments with debris flows of ~ 10 m^3 of water-saturated sand and gravel (with 2% silt and clay by weight) were conducted at the USGS debris flow flume which is a rectangular concrete chute 95 m long and 2 m wide that slopes 31° throughout most of its length and flattens at its base to adjoin a runout surface that slopes 2.5°. The solid-water mixture was initially placed as a triangular wedge against a vertical gate of 2m height, and suddenly released by the gate opening. In the experiment, the flow was confined by concrete panels which effectively extended the flow length 7.4m across the runout surface. Details of the flume facility and experimental methods have been reported in Iversion (1997). Numerical computation has been conducted using the debris properties of ρ = 2000 kg /m^3 , C_Z = 37$m^{1/2}$ s , θ = 31°, and Φ = 7°. The computational domain is discretized using 841 grid points and the computational time-step is set with a CLF number of 0.9.

Flow depths computed at locations 2 m, 33 m, and 67 m downstream of the vertical gate are compared with experimental measurements and previously simulated results of Denlinger & Iverson (2001) in Fig. 1. As also observed in solutions of Denlinger and Iverson, the most significant simulation errors occur at the location 2m downstream of the gate. As already pointed out by Denlinger & Iverson, it is because the depth-averaged model does not account for reaction forces exerted by the static bed in response to the slope-normal acceleration, and it consequently predicts too much thinning just downstream of the gate.

Further downstream of the gate, however, the computed results reveals that present numerical model can reasonably well reproduce the flow.

COMPARISON OF FLOOD AND DEBRIS FLOWS

Understanding and modelling the flow behaviour of flood flow and debris flow is a crucial prerequisite for the development of the design criteria of culverts in the debris flow potential regions. Laboratory experiments are presented that model the debris flows with

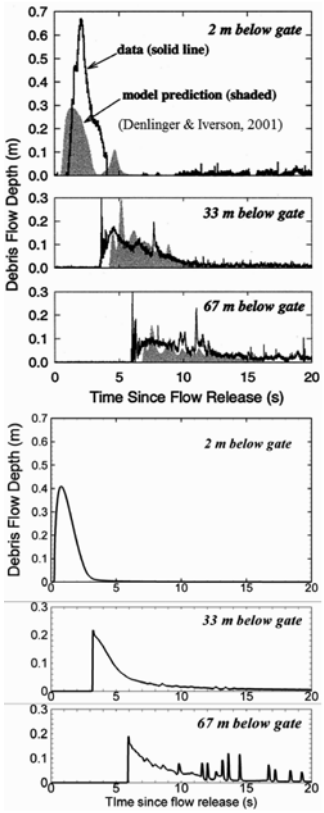

Fig.1 - Comparison of [upper] measurement and prediction of Denlinger & Iverson (2001) with [lower] present prediction

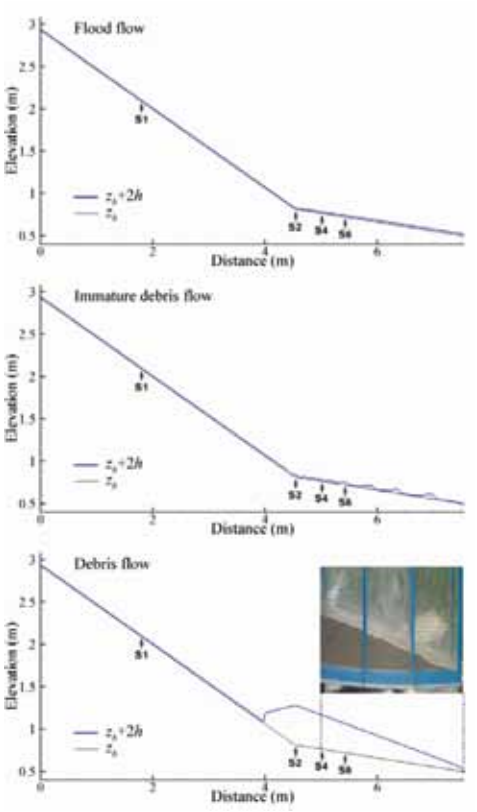

Fig .2 - Computed depth profiles of (upper) flood flow, (centre) immature debris flow, and (lower) debris flow at t = 120s

various fluid-solid mixtures in a rectangular channel which consists of two channel of different slope angles: the upstream channel of 5 m length and 25° slope and the downstream channel of the length of 3 m and a bed slope of 6° including a culvert at various angles. The measurement methods include six ultrasonic sensors to measure flow depth and record stage hydrographs and video cameras to assess the surface velocity and interpret the flow processes of debris flows. The experimental measurements show that the flow depth of debris flows dramatically increase as compared with that of the clear water flow, and depends on the angle of culvert slope as well as the sediment concentration. We calculate a flood flow, a immature debris flow and a debris flow in the experimental flume using flow resistance relations of Eq. (3), Eq(4) and Eq. (5), respectively. Based on the calibration and the test of material properties, the manning coefficient n in Eq. (3) is set to be 0.01 s $m^{-1/3}$ while the Chezy coefficient in Eq. (5) equals to 44.0 $m^{1/2}$ s . The effective mean particle diameter in the immature debris flow relataion is set to be 0.8mm based on the particle size analysis. The total simulation time is 120 s and the time step is specified at every time with a CFL number of 0.6.

Depth profiles for three different flows computed at the time of 120 s at the same flow rate are compared in Fig. 2 where the flow depth is doubled for visualization. As shown in the figure, the fresh water flow, computed flow depth is appeared to increase by 40% at the downstream channel. Note the overall longitudinal depth profile of flood flow shown in Fig. 2(a) is in very good agreement with the experimental measurement. Interestingly, the numerical result of an immature debris flow reveals the emergence of the debris flow surge as shown in Fig. 2(b). This kind of debris flow surges were experimentally investigated by Davies (1990). Consequently, the local depth of the immature debris flow significantly increased, but the deposition of sediments in the downstream channel was not observed in the numerical results. In contrast,

the numerical results obtained by using the Voellmy relations shows that the typical debris flow results in the significant deposition of sediments in the downstream culvert of low bed slope. The computed debris flow deposition is in good agreement with our flow visualization shown in inset, as shown in Fig. 2(c).

We further compared the computed time history of debris flow deposition at four different locations with experimental measurements obtained by ultrasonic sensors in Fig. 3. As shown in the figure, the patterns of sediment deposition in the computed flow field are different from those of the measurements. It is because of the assumption of a complete single phase flow for the debris flow in the computation. It should be note, however, that the final deposition depth computed based on the single phase flow is comparable to the experimental measurements. This result provide useful information on the debris flow transient through culverts.

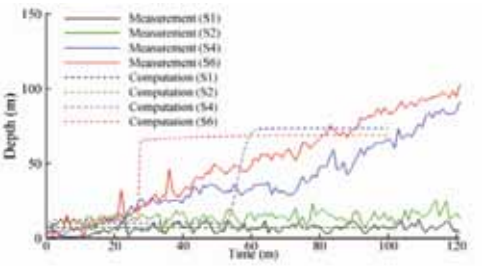

Fig. 3 - Experimental measurements (solid lines) and numerical predictions (dashed lines) at four different sections (see Fig. 2 for section numbers, S1- S6)

CONCLUSIONS

A 1D debris flow model based on the shallow water equations with complex source terms has been developed to simulate 1D non- Newtonian debris flows. Three flow resistance relations for the flood flow, immature debris flow and debris flows are incorporated into the model to investigate the time-dependent behaviours of such flows in the culvert-like channel of low bed angle. The governing equations are solved by a second-order-accurate finite volume method employing Godunov-type schemes with spatially discretized flux functions and TVD-limiters for high-resolution monotone solutions.

To evaluate the numerical model, we first apply it to calculate a saturated debris flow in a large scale experimental channel. The comparison of the numerical results with experimental measurements shows that the present model can reasonably well reproduce laboratory but fairly large scale debris flows. To investigate the behaviour of the common flood flow, an immature debris flow and debris flow in our laboratory flume with a square culvert and an abrupt change of bed slope, we conducted these flows using corresponding flow resistance relations. The numerical results appear to be in good agreement with our experimental measurements which provide useful information on the debris flow transient through culverts. The numerical results show that the present model is a promising engineering tool for practical simulations of such flows. We elucidate the transient features of flood and debris flows through culverts, based on numerical solutions of such flows in the open channel with culvert at various configurations of different bottom slopes between the channel and the culvert

ACKNOWLEDGEMENTS

This research was financially supported by a grant (Code#'08 RTIP B-01, RD-Flow Project) from Regional Technology Innovation Program funded by the Ministry of Land, Transport and Maritime Affairs of Korean Government..

REFERENCES

Bertolo P. & Wieczorek G.F. (2005) - *Calibration of numerical models for small debris flows in Yosemite Valley, California, USA.* Natural Hazards and Earth System Sciences, **5**: 993-1001.

Brufau P., García-Navarro P., Ghilardi P., Natale I. & Savi F. (2000*) - 1D mathematical modeling of debris flow.* J. Hydraul. Res., **38**: 435-446.

Davies T.R.H. (1990) - *Debris-flow surges-experimental simulation.* J. Hydrology (NZ), **29**(1): 18-46.

Denlinger R.P. & Iverson R.M. (2001*) - Flow of variably fluidized granular masses across three-dimensional terrain: 2. Numerical predictions and experimental tests.* J. Geophys. Res., **106**(B1): 553-566.

Julien P.Y .& Leon C. (2000) - *Mudfloods, mudflows and debris flows, classification in rheology and structural design.* Proc. Int. Workshop on the Debris Flow Disaster of December 1999 in Venezuela, Universidad Central de Venezuela, Caracas,

Venezuela.

Liang Q. & Marche F. (2009) - *Numerical resolution of well-balanced shallow water equations with complex source terms.* Advanced in Water Resources, **32**: 873-884.

Medina V., Hürlimann M.,& Bateman A., (2008) - *Application of FLATModel, a 2D finite volume code, to debris flows in the northeastern part of the Iberian Peninsula.* Landslides, **5**: 127-142.

Naef D., Rickenmann D., Rutschmann P., & McArdell B.W. (2006) - *Comparison of flow resistance relations for debris flows using a onedimensional finite element simulation model.* Natural Hazards and Earth System Sciences, **6**: 155-165.

Paik J., Park S.-D. & Yoon Y.-H. (2010) - *A shock-capturing method for 1D debris flows.* IAHR-APD2010 Conference Proceeding, February 21-24, Auckland, New Zealand,

Takahashi T. (1991*) - Debris Flow.* A.A. Balkema, Rotterdam.

Toro E.F. (2001) - *Shock-Capturing Methods for Free-Surface shallow flows.* John Wiley & Sons, LTD, Baffins Lane, Chichester, England.

Varnes D.J. (1978*) - Slope movement types and processes.* In: Schuster R.L. & Krizek R.J. (eds)*, Landslides: Analysis and Control* (Transportation Research Board Special Report 176: 11-33). National Academy of Sciences, Washington, DC.

